Atmos. Chem. Phys. Discuss., 12, 12485–12502, 2012
www.atmos-chem-phys-discuss.net/12/12485/2012/
doi:10.5194/acpd-12-12485-2012

Atmospheric Chemistry and Physics Discussions

On the interpretation of an unusual in-situ measured ice crystal scattering phase function

A. J. Baran[1], J.-F. Gayet[2], and V. Shcherbakov[2,3]

[1]Met Office, FitzRoy Road, Exeter, EX1 3PB, UK
[2]Laboratoire de Météorologie Physique,UMR6016 CNRS/Université Blaise Pascal, Clermont-Ferrand, France
[3]Laboratoire de Météorologie Physique, Institut Universitaire de Technologie d'Allier, Montluçon, France

Received: 3 May 2012 – Accepted: 3 May 2012 – Published: 15 May 2012

Correspondence to: A. J. Baran (anthony.baran@metoffice.gov.uk)

Published by Copernicus Publications on behalf of the European Geosciences Union.

Abstract

In-situ Polar Nephelometer (PN) measurements of unusual ice crystal scattering phase functions were recently reported by Gayet et al. (2012). The ice crystal habits that produced the phase functions were small chain-like aggregates, which had on their surfaces, smaller quasi-spherical ice crystals. The measured-averaged phase functions were featureless, at scattering angles less than about 100°, but an ice bow-like feature was noted between the scattering angles of about 120° to 160°. The estimated asymmetry parameter was 0.78 ± 0.04.

In this paper, the phase function is interpreted in terms of a weighted habit mixture model. The best-fit model comprises of highly distorted ten element hexagonal ice aggregates, and the smaller quasi-spherical ice crystals are represented by Chebyshev ice particles. The weighted mean asymmetry parameter was found to be 0.81. It is argued that the Chebyshev-like ice particles are responsible for the ice bow-like feature and mostly dominate the scattered intensity measured by the PN. The results of this paper have important implications for climate modelling (energy balance of anvils) and the remote sensing of cirrus properties.

1 Introduction

The most-recent report of the Intergovernmental Panel on Climate Change (IPCC, 2007) concluded that radiative coupling, between clouds of all types, and the Earth's atmosphere is still one of the greatest uncertainties in predicting climate change. One such cloud-type that exacerbates this uncertainty is cirrus. This is because cirrus is composed of highly irregular ice crystals, which generally exist as various habit mixtures, and their sizes can vary between less than 10 µm toward the cloud-top, to several centimetres toward the cloud-bottom (Baran, 2009).

Due to this variability in ice crystal size and shape, using climate models to predict the radiative effect of cirrus has proven to be problematic (Zhang et al., 1999;

ACPD
12, 12485–12502, 2012

Kristjánsson et al., 2000; Edwards et al., 2007; and Gu et al., 2011). These modelling studies have shown that the net radiative effect of cirrus can be neutral, negative (i.e., cools the Earth's surface) or positive (i.e., warms the Earth's surface). The short-wave radiative effect can vary from about $-30\,\mathrm{W\,m^{-2}}$ to about $-70\,\mathrm{W\,m^{-2}}$ depending on model assumptions (Baran, 2009). This large range in the short-wave radiative effect is due to the uncertainty in the scattering properties of ice crystals (Baran, 2004; Ulanowski et al., 2006; Fu, 2007; Yang et al., 2008; Baran, 2009; Gayet et al., 2011, 2012). However, in recent years there has been a large amount of research that has focused on habit mixture models of cirrus and their bulk-scattering properties (Macke et al., 1996a; Mishchenko et al., 2002; Baum et al., 2005, 2011; Baran and Labonnote, 2007; Baran, 2012, and references therein).

Clearly, to improve cirrus parameterization in climate models, understanding the scattering properties of highly irregular ice crystals is of paramount importance, if the uncertainty about the net radiative effect of cirrus is to be reduced. However, such understanding is not only important for climate models but also for the space-based remote sensing of cirrus properties (Mishchenko et al., 1996; Baran et al., 1999; Yang et al., 2008; McFarlane et al., 2005; Ulanowski et al., 2011).

One scattering property that is of fundamental importance in the remote sensing of cirrus microphysical and macrophysical properties is the scattering phase function (i.e., the angle-dependent scattered intensity about the ice crystal) (van de Hulst, 1957). Application of an inappropriate phase function can lead to significant errors in the retrieval of optical thickness and/or ice crystal size (Mishchenko et al., 1996; Baran et al., 1999; Yang et al., 2008). Therefore, there is a need to constrain the scattering phase function of cirrus. Currently, passive radiometric observational evidence suggests that the best scattering phase functions to represent cirrus are those which are featureless and relatively flat at backscattering angles (Foot, 1988; Francis et al., 1999; Baran et al., 1999, 2001; Labonnote et al., 2001; Jourdan et al., 2003; Baran and Labonnote, 2006, 2007; Baum et al., 2011).

ACPD
12, 12485–12502, 2012

Title Page
Abstract | Introduction
Conclusions | References
Tables | Figures
◀◀ | ▶▶
◀ | ▶
Back | Close
Full Screen / Esc
Printer-friendly Version
Interactive Discussion

However, Gayet et al. (2012) reported the in-situ measurement of an unusual scattering phase function of ice crystals in a mid-latitude anvil cloud, towards the cloud-top. The habits responsible for the measured phase functions consisted of small chain-like aggregates, which had on each monomer that made up the chain, smaller quasi-spherical ice crystals.

The scattering phase function reported by Gayet et al. (2012) is unusual in that it was featureless at scattering angles less than about 100°, but had an ice bow-like feature between the scattering angles of about 120° to 160°. Therefore, this measured in-situ phase function was not relatively flat at backscattering angles. The scattering phase function measurements reported by Gayet et al. (2012) brings into question the generality of supposing relatively flat ice crystal scattering phase functions at backscattering angles. In this paper, the phase function reported by Gayet et al. (2012) is theoretically interpreted in terms of a best-fit habit mixture model of ice crystals. The paper is split into the following sections. Section 2 gives a brief discussion of the original measurements, Sect. 3 describes the theoretical methodology used to interpret the PN measurements, and Sect. 4 discusses the results. Section 5 presents the conclusions.

2 The measurements

In this paper, the phase function measurements reported by Gayet et al. (2012) are used, and in that paper they are comprehensibly described. However, a very brief description of the most pertinent measurements to this paper is given. The measurements were obtained during the CIRCLE-2 experiment, which was carried out over Western Europe during May 2007. During this experiment, a combination of in-situ microphysical and remote-sensing measurements was obtained in, and above, an overshooting convective cell. The measurements used throughout this paper, were obtained near the cloud-top, at temperatures of about −58 °C. During the CIRCLE-2 campaign, the PN instrument was available (Gayet et al., 1998). As the ice crystals enter the sampling volume of the PN, they are intersected by a collimated laser beam, operating

ACPD
12, 12485–12502, 2012

at 0.80 µm, near the focal point of a paraboloidal mirror. A circular array of 54 diodes measure the scattered intensity of laser light scattered at polar angles between 15° and 162°, by each crystal so illuminated. A microphysical probe used during the CIRCLE-2 experiment was the Cloud Particle Imager (CPI) (Lawson et al., 2001). The CPI was used to image the ice crystal habits, and estimate their sizes, example images of the ice crystal habits, imaged near the cloud-top, are shown in Fig. 1.

The figure shows that the ice crystal habits appeared to consist of chains of aggregates, with maximum dimensions ranging between about 100 µm to about 400 µm. Although, the appearance of chain-like aggregates has been previously reported (Saunders and Wahab, 1975; Connolly et al., 2005; Um and McFarquhar, 2009; Baran, 2009; Gayet et al., 2012), their corresponding scattering phase functions have not generally been measured, until Gayet et al. (2012). The PN measured the scattering phase function for each of the ice crystals shown in Fig. 1, and the measured average scattering phase function, near the cloud-top, is shown in Fig. 7c of Gayet et al. (2012), and the PN estimated-averaged asymmetry parameter was found to be 0.78 ± 0.04. The asymmetry parameter, g, is formally defined as the average cosine of the polar (scattering) angle, and is therefore, a measure of the degree of asymmetry in the forward scattering part of the phase function. The asymmetry parameter can take on values between ± 1.0. It is a very important parameter to constrain in climate models because it determines how much incident sunlight is reflected back to space (Stephens and Webster, 1981; Liou and Takano, 1994; Baran, 2004; Ulanowski et al., 2006).

In the paper by Gayet et al. (2012) it is shown that the measured-averaged phase function, at scattering angles less than about 100°, is featureless. Which corresponds to previous reports that the measured scattered intensity of more complex ice crystals do not exhibit halo features, around the scattering angles of 22° and 46° (Field et al., 2003; Ulanowski et al., 2011; Gayet et al., 2011, 2012). However, at scattering angles between about 120° and 160°, there appears a bow-like feature. The appearance of bow-like features on the scattering phase function, at backscattering angles, is contrary to the general radiometric measurements discussed in Sect. 1. Moreover, Gayet et al. (2012) also noted the presence of much smaller quasi-spherical ice particles on the surfaces of the aggregate-chains. The possibility of the bow-like feature being due to the surface quasi-spherical ice particles rather than the underlying crystal shape is discussed in Sect. 4.

3 Theoretical methodology

To interpret the scattering phase function reported by Gayet et al. (2012), a number of light scattering methods are used. Firstly, in the rest of this paper, the ice crystals are assumed to be randomly oriented, and the incident wavelength is 0.80 µm. The refractive index of ice at this wavelength is $1.3049 + i1.34 \times 10^{-7}$ (Warren and Brandt, 2008), where i is the imaginary part.

To compute the scattering phase function (first element in the first column of the scattering matrix [1,1], see van de Hulst, 1957), $P_{11}(\theta)$, and g for each ice crystal, the methods of Monte-Carlo ray tracing (Macke et al., 1996a) and T-matrix (Mishchenko and Travis, 1998) are applied. The method of ray-tracing is applied to a model chain of aggregates, and the T-matrix method is applied to rotationally symmetric particles, which represent the quasi-spherical particles. Since no halo features are noted on the averaged scattering phase function reported by Gayet et al. (2012), the method of distortion is applied to the ray tracing (Macke et al., 1996a). In this method, at each refraction and reflection event, the ray-paths are randomly tilted, with respect to their original direction. This randomization process removes energy from the halo and ice bow regions and re-distributes it to side-scattering and backscattering angles. Therefore, for high distortion parameters, the halo and ice bow features are removed, creating featureless phase functions. The distortion parameter can have values ranging from 0 (i.e., no distortion) to 1.0 (i.e., maximum distortion). Other methods to remove halos and ice bows include surface roughness (Yang and Liou, 1998; Ulanowski et al., 2006) and including ice crystals with spherical air inclusions and/or aerosol (Macke et al., 1996b; Labonnote et al., 2001) or a combination of distortion and spherical air inclusions (Baran and Labonnote, 2007). These methods of randomization decrease the asymmetry parameter of the model ice crystal, with respect to their pristine counterparts (Yang and Liou, 1998; Ulanowski et al., 2006).

The chain of aggregates shown in Fig. 1 is represented by a ten-element hexagonal ice aggregate, previously described by Baran and Labonnote (2007), see Fig. 1f of that paper. The quasi-spherical particles are represented by rotationally symmetric spheroids and Chebyshev ice particles. The geometries of these particles have previously been described by (Mugnai and Wiscombe, 1986; Mishchenko and Travis, 1998). To retain the ice bow feature, the quasi-spherical particles are assumed to have the following geometrical parameters. The aspect ratios (i.e., ratio of horizontal semi-axis to rotational semi-axis), R, of the prolate and oblate spheroids are assumed to be 0.8333 and 1.2 (R as defined by Mishchenko and Travis, 1998), respectively, and the equal-area spherical radius is assumed to be 12 µm. The Chebyshev particles are assumed to be of order 3, have an unperturbed spherical radius of 12 µm, and deformation parameters of 0.03, and 0.1. Hereinafter, the two Chebyshev particles are described by the term $Tn(\varepsilon)$, where n is the Chebyshev order, and ε is the deformation parameter, as defined by Mishchenko and Travis (1998).

To simulate the measured averaged scattering phase function, three weighted habit mixture models are investigated. A weighted habit mixture model is assumed because, currently, there is no one single electromagnetic method that can solve the scattering properties of chain aggregates for the sizes shown in Fig. 1. The first weighted habit mixture model is comprised of two Chebyshev ice particles, called model 1. The second model consists of the ten-element hexagonal ice aggregate and prolate and oblate spheroids, called model 2. The third model consists of the ten-element hexagonal ice aggregate and the two Chebyshev ice particles, called model 3. The weighted mean habit mixture phase function model, $\overline{P_{11}(\theta)}$, is given by:

$$\overline{P_{11}(\theta)} = \sum_{j=1}^{j=N} w_j P_j(\theta) \tag{1}$$

Discussion Paper | Discussion Paper | Discussion Paper | Discussion Paper |

ACPD

12, 12485–12502, 2012

Unusual in-situ measured ice crystal scattering phase function

A. J. Baran et al.

where in Eq. (1), w_j is the weighting applied to each phase function, $P_j(\theta)$, where the subscript 11 has been dropped to aid clarity, and values for θ are between 0° and 180°. Throughout this paper the phase functions are normalized to 4π. By definition $\Sigma w_j = 1$. Similarly, the weighted mean asymmetry parameter, $\overline{g}$, is given by

$$\overline{g} = \sum_{j=1}^{j=N} w_j g_j. \tag{2}$$

In Eq. (1), the weights are found by minimizing the root mean square error (rmse), X_{rmse}, which is defined by:

$$X_{\text{rmse}} = \sqrt{(1/N)\left\{\sum_{i=1}^{i=32} X_i^2\right\}} \tag{3}$$

where in Eq. (3), X_i is the difference between the measured average phase function and $\overline{P_{11}(i)}$, where $i = 1\ldots N$, and $N = 32$ (i.e., the number of scattering angles measured by the PN).

4 Results

To compare the experimental and model phase functions, both are normalized to unity at the scattering angle of 15°, therefore, comparisons are made in terms of the shape of the scattering phase functions, over the full range of the measured angular domain. Considering model 1, and using Eqs. (1) and (3), the best weighted habit mixture model was found to be:

$$\overline{P_{11}} = 0.4P_{11}^{T3(0.03)} + 0.6P_{11}^{T3(0.1)} \tag{4}$$

ACPD
12, 12485–12502, 2012

where i has been dropped for reasons of clarity. Comparisons between $\overline{P_{11}}$ and the measured phase function are shown in Fig. 2. The figure shows that for scattering angles between about 15° and 40°, model 1 does describe the forward scattering part of the measured phase function. However, at side-scattering angles between about 60° and 120°, the model severely underpredicts the measurements. However, the ice bow feature, between the scattering angles of 120° and 160°, is predicted by the Chebyshev particle model, though underpredicted. Therefore, Fig. 2 demonstrates that quasi-spherical particles alone cannot explain the measured phase function. Moreover, $\overline{g}$ predicted by model 1 is 0.84, which is outside the upper range of uncertainty estimated by the PN. A Phase function with higher side scattering is required, without halo features, which can only be predicted by an irregular ice crystal model.

To obtain a phase function with higher side scattering, without halo features, the highly distorted ten element hexagonal ice aggregate is now considered. To reduce the noise in the Monte-Carlo ray tracing calculations for each phase function, the phase functions were averaged over four maximum dimensions, which were 100 µm, 200 µm, 400 µm and 600 µm. For each maximum dimension, the overall aspect ratio of the ten element hexagonal ice aggregate remained invariant with respect to size. A distortion parameter of 0.8 was assumed for all four Monte-Carlo ray tracing calculations. It should be noted here that the averaged g value found for the ten element hexagonal ice aggregate was 0.68.

Considering model 2, the best weighted habit mixture model was found to be

$$\overline{P_{11}} = 0.2P_{11}^{\text{ice aggregate}} + 0.3P_{11}^{\text{prolate}(R=0.83333)} + 0.5P_{11}^{\text{oblate}(R=1.2)}. \tag{5}$$

The results of comparing this phase function with the measured phase function is shown in Fig. 3. Clearly, the figure shows that the addition of the highly distorted ten element hexagonal ice aggregate has improved the fit between model 2 and the measured phase functions, relative to model 1, especially between the scattering angles of about 40° and 160°. However, the peak in the ice bow assuming spheroids occurs at a scattering angle of about 130°, compared to the measured peak, which is at about

ACPD
12, 12485–12502, 2012

140°. The predicted weighted habit $\overline{g}$ value for model 2 was found to be 0.83, which is just outside the upper range of uncertainty estimated by the PN.

For model 3, the best fit model phase function to the measured phase function was found to be

$$\overline{P_{11}} = 0.2P_{11}^{\text{ice aggregate}} + 0.5P_{11}^{T3(0.03)} + 0.3P_{11}^{T3(0.1)}. \quad (6)$$

and the comparison between the measured phase function and $\overline{P_{11}}$ is shown in Fig. 4. The figure shows that this model better captures, relative to the other models, the shape of the measured phase function between the scattering angles of about 100° and 160°, even predicting the peak of the measured ice bow feature at the correct scattering angle. However, the model slightly underpredicts the measured phase function at scattering angles between about 60° and 95°. The predicted $\overline{g}$ value for model 3 was found to be 0.81, which is within the upper range of uncertainty estimated by the PN. The rmse for model 3 was found to be 0.017, whilst for model 2 it was 0.029.

5 Conclusions

In this paper, an unusual in-situ measured phase function has been interpreted in terms of a weighted habit mixture model. The best-fit habit mixture model found, comprised of a highly distorted ten element hexagonal ice aggregate, and two Chebyshev particles of order 3. A distortion parameter of 0.8 was applied to the ten element hexagonal ice aggregate, and the Chebyshev ice particles were each assumed to have an unperturbed spherical radius of 12 µm, and deformation parameters of 0.03 and 0.1, and the best-fit weightings were estimated to be 0.2, 0.5, and 0.3, respectively. The best-fit $\overline{g} = 0.81$, which compares to the estimated PN asymmetry parameter value of 0.78 ± 0.04, therefore, $\overline{g}$ is within the upper range of the experimental uncertainty.

The best-fit model demonstrates that the measured ice bow, assuming highly distorted ice crystals, can be predicted assuming quasi-spherical particles. Therefore, it is

ACPD
12, 12485–12502, 2012

the quasi-spherical particles that dominate the scattering measured by the PN, rather than the underlying chain-aggregate, although these must be randomized to produce sufficient side scattering and remove halo features. Moreover, Figs. 3 and 4 demonstrate that the full range of scattering angle needs to be measured at sufficient resolution to estimate values for the asymmetry parameter. It can no longer be generally assumed that phase functions with no halos are also featureless and relatively flat at backscattering angles. This may be particularly true for the tops of anvil cloud, and for this type of cloud the asymmetry parameter is particularly important. The findings of this paper have important implications for climate modelling and for the remote sensing of cirrus. It is therefore of necessity to understand whether the phase functions, and consequently, their asymmetry parameters, shown throughout this paper are a common occurrence.

Acknowledgements. The CIRCLE-2 experiment was funded by the Centre National d'Etudes Spatiales (CNES) and by a grant from the CNRS/INSU. The contribution of DLR as well as large part of Falcon flight hours was funded in the framework of the DLR PAZI-2 project.

References

Baran, A. J.: On the scattering and absorption properties of cirrus cloud, J. Quant. Spectrosc. Ra., 89, 17–36, 2004.

Baran, A. J.: A review of the light scattering properties of cirrus, J. Quant. Spectrosc. Ra., 110, 1239–1260, 2009.

Baran, A. J.: From the single-scattering properties of ice crystals to climate prediction: A way forward, Atmos. Res., 112, 45–69, 2012.

Baran, A. J. and Labonnote, L.-C.: On the reflection and polarization properties of ice cloud, J. Quant. Spectrosc. Ra., 100, 41–54, 2006.

Baran, A. J. and Labonnote, L.-C.: A self-consistent scattering model for cirrus. 1: the solar region, Q. J. Roy. Meteor. Soc., 133, 1899–18912, 2007.

ACPD
12, 12485–12502, 2012

Baran, A. J., Watts, P. D., and Francis, P. N.: Testing the coherence of cirrus microphysical and bulk properties retrieved from dual-viewing multispectral satellite radiance measurements, J. Geophys. Res., 104, 31673–31683, 1999.
Baum, B. A., Heymsfield, A. J., Yang, P., and Bedka, S. T.: Bulk scattering properties for the remote sensing of ice clouds. Part I. Microphysical data and models, J. Appl. Meteorol., 44,1885–1895, 2005.
Baum, B. A., Yang, P., Heymsfield, A. J., Schmitt, C. G., Xie, Y., Bansemer, A., Hu, Y.-X., Zhang, Z.: Improvements in shortwave bulk scattering and absorption models for the remote sensing of ice clouds, J. Appl. Meteorol. Clim., 50, 1037–1056, 2011.
Connolly, P. J., Saunders, C. P. R., Gallagher, M. W., Bower, K. N., Flynn, M. J., Choularton, T. W., Whiteway, J., and Lawson, R. P.: Aircraft observations of the influence of electric fields on the aggregation of ice crystals, Q. J. Roy. Meteor. Soc., 128, 1–19, 2005.
Edwards, J. M., Havemann, S., Thelen J.-C., and Baran, A. J.: A new parametrization for the radiative properties of ice crystals: comparison with existing schemes and impact in a GCM, Atmos. Res., 83, 19–35, 2007.
Field, P. R., Baran, A. J., Kaye, P. H., Hirst, E., and Greenaway, R.: A test of cirrus ice crystal scattering phase functions, Geophys. Res. Lett., 30, 1752, doi:10.1029/2003GL017482, 2003.
Foot, J. S.: Some observations of the optical properties of clouds, II: cirrus, Q. J. Roy. Meteor. Soc., 114, 141–164, 1988.
Francis, P. N., Foot, J. S., and Baran, A. J.: Aircraft measurements of the solar and infrared radiative properties of cirrus and their dependence on ice crystal shape, J. Geophys. Res., 104, 31685–31695, 1999.
Fu, Q.: A new parameterization of an asymmetry factor of cirrus clouds for climate models, J. Atmos. Sci., 64, 4140–4150, 2007.
Gayet, J.-F., Auriol, F., Oshchepkov, S., Schröder, F., Duroure, C., Febvre, G., Fournol, J.-F., Crépel, O., Personne, P., and Daugeron, D.: In-situ measurements of the scattering phase function of stratocumulus, contrails and cirrus, Geophys. Res. Lett., 25, 971–974, 1998.
Gayet, J.-F., Mioche, G., Shcherbakov, V., Gourbeyre, C., Busen, R., and Minikin, A.: Optical properties of pristine ice crystals in mid-latitude cirrus clouds: a case study during CIRCLE-2 experiment, Atmos. Chem. Phys., 11, 2537–2544, doi:10.5194/acp-11-2537-2011, 2011.
Gayet, J.-F., Mioche, G., Bugliaro, L., Protat, A., Minikin, A., Wirth, M., Dörnbrack, A., Shcherbakov, V., Mayer, B., Garnier, A., and Gourbeyre, C.: On the observation of unusual

high concentration of small chain-like aggregate ice crystals and large ice water contents near the top of a deep convective cloud during the CIRCLE-2 experiment, Atmos. Chem. Phys., 12, 727–744, doi:10.5194/acp-12-727-2012, 2012.
Gu, Y., Liou, K. N., Ou, S. C., and Fovell, R.: Cirrus cloud simulations using WRF with improved radiation parameterization and increased vertical resolution, J. Geophys. Res., 116, D06119, doi:10.1029/2010JD014574, 2011.
van de Hulst, H. C.: Light Scattering by Small Particles, Wiley, New York, 1957.
Intergovernmental Panel on Climate Change: Climate Change 2007 – The Physical Science Basis: Contribution of Working Group I to the Fourth Assessment Report of the IPCC, Cambridge University Press, Cambridge, 2007.
Jourdan, O., Oshchepkov, S., Shcherbakov, V., Gayet, J.-F., and Isaka, H.: Assessment of cloud optical parameters in the solar region: retrievals from airborne measurements of scattering phase functions, J. Geophys. Res., 108, 4572, doi:10.1029/2003JD003493, 2003.
Kristjánsson, J. E., Edwards, J. M., and Mitchell, D. L.: The impact of a new scheme for the optical properties of ice crystals on the climate of two GCMs, J. Geophys. Res., 105, 10063–10079, 2000.
Labonnote, L. C., Brogniez, G., Buriez, J.-C., Doutriaux-Boucher, M., Gayet, J.-F., and Macke, A.: Polarized light scattering by inhomogeneous hexagonal monocrystals. Validation with ADEOS-POLDER measurements, J. Geophys. Res., 106, 12139–12153, 2001.
Lawson, R. P., Baker, B. A., Schmitt, C. G. and Jensen, T. L.: An overview of microphysical properties of Arctic clouds observed in May and July 1998 during FIRE.ACE., J. Geophys. Res., 106, 14989–15014, 2001.
Liou, K.-N. and Takano, Y.: Light scattering by nonspherical particles: remote sensing and climatic implications, Atmos. Res., 31, 271–298, 1994.
Macke, A., Mueller, J., and Raschke, E.: Single scattering properties of atmospheric ice crystal, J. Atmos. Sci., 53, 2813–2825, 1996a.
Macke A., Mishchenko, M. I., and Cairns, B.: The influence of inclusions on light scattering by large particles, J. Geophys. Res., 101, 23311–23316, 1996b.
McFarlane, S. A., Marchand, R. T., and Ackerman, T. P.: Retrieval of cloud phase and crystal habit from Multiangle Imaging Spectroradiometer (MISR) and Moderate Resolution Imaging Spectroradiometer (MODIS) data, J. Geophys. Res., 110, D14201, doi:10.1029/2004JD004831, 2005.

Mishchenko, M. I. and Travis, L. D.: Capabilities and limitations of a current FORTRAN implementation of the T-matrix method for randomly oriented rotationally symmetric scatterers, J. Quant. Spectrosc. Ra., 60, 309–324, 1998.
Mishchenko, M. I., Rossow, W., Macke, A., and Lacis, A. A.: Sensitivity of cirrus cloud albedo, bidirectional reflectance and optical thickness retrieval accuracy to ice particle shape, J. Geophys. Res., 101, 16973–1698, 1996.
Mishchenko, M. I., Travis, L. D., and Lacis, A. A.: Scattering, Absorption, and Emission of Light by Small particles, Cambridge University Press, Cambridge, 2002.
Mugnai A. and Wiscombe W. J.: Scattering from nonspherical Chebyshev particles. I: Cross sections, single-scattering albedo, asymmetry factor and backscattering fraction, Appl. Optics, 25, 1235–1244, 1986.
Saunders, C. P. R. and Wahab, N. M. A.: The influence of electric fields on the aggregation of ice crystals, J. Meteorol. Soc. Jpn., 53, 121–126, 1975.
Stephens, G. L. and Webster, P. J.: Clouds and climate: sensitivity of simple systems, J. Atmos. Sci., 38, 235–245, 1981.
Ulanowski, Z., Hesse, E., Kaye, P. H., and Baran, A. J.: Light scattering by complex ice-analogue crystals, J. Quant. Spectrosc. Ra., 100, 382–392, 2006.
Ulanowski, Z., Kaye, P. H., Hirst, E., and Greenaway, R.: Retrieving the size of particles with rough surfaces from 2-D scattering patterns, in: 13th Int. Conf. on Electromagnetic & Light Scatt., 26–30 September 2011, Taormina, doi:10.1478/C1V89S1P087, 2011.
Um, J. and McFarquhar, G. M.: Single-scattering properties of aggregates plates, Q. J. Roy. Meteor. Soc., 135, 291–304, 2009.
Warren, S. G. and Brandt, R. E.: Optical constants of ice from the ultraviolet to the microwave: a revised compilation, J. Geophys. Res., 113, D14220, doi:10.1029/2007JD009744, 2008.
Yang, P. and Liou, K. N.: Single-scattering properties of complex ice crystals in terrestrial atmosphere, Contr. Atmos. Phys., 71, 223–248, 1998.
Yang, P., Zhang, Z. B., Kattawar, G. W.,Warren, S. G., Baum, B. A., Huang, H. J., Hu, Y. X., Winker, D., and Iaquinta, J.: Effect of cavities on the optical properties of bullet rosettes: implications for active and passive remote sensing of ice cloud properties, J. Appl. Meteorol. Clim., 47, 2311–2330, 2008.
Zhang, Y., Macke, A., and Albers, F.: Effect of crystal size spectrum and crystal shape on stratiform cirrus radiative forcing, Atmos. Res., 52, 59–75, 1999.

ACPD
12, 12485–12502, 2012

Unusual in-situ measured ice crystal scattering phase function

A. J. Baran et al.

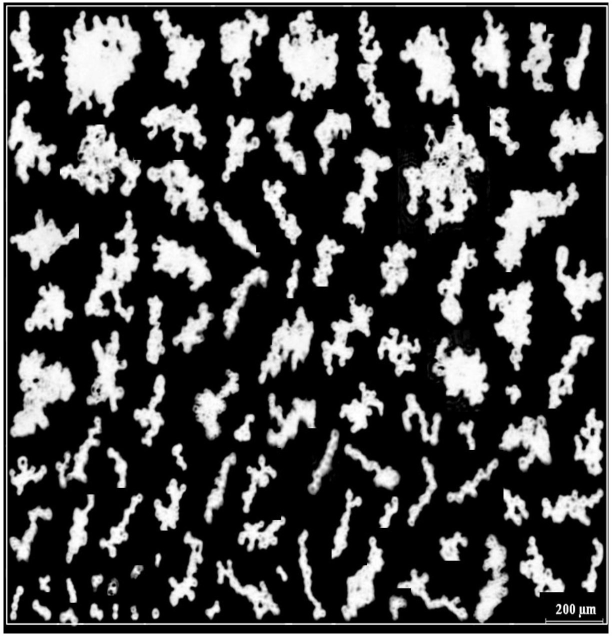

Fig. 1. CPI example images of ice crystal chain-aggregates that occurred near the cloud-top of an overshooting mid-latitude anvil, obtained during the CIRCLE-2 experiment. The ice crystal size is shown by the scale located at the bottom-right-hand-side of the figure. From Gayet et al. (2012), see their Fig. 8.

ACPD
12, 12485–12502, 2012

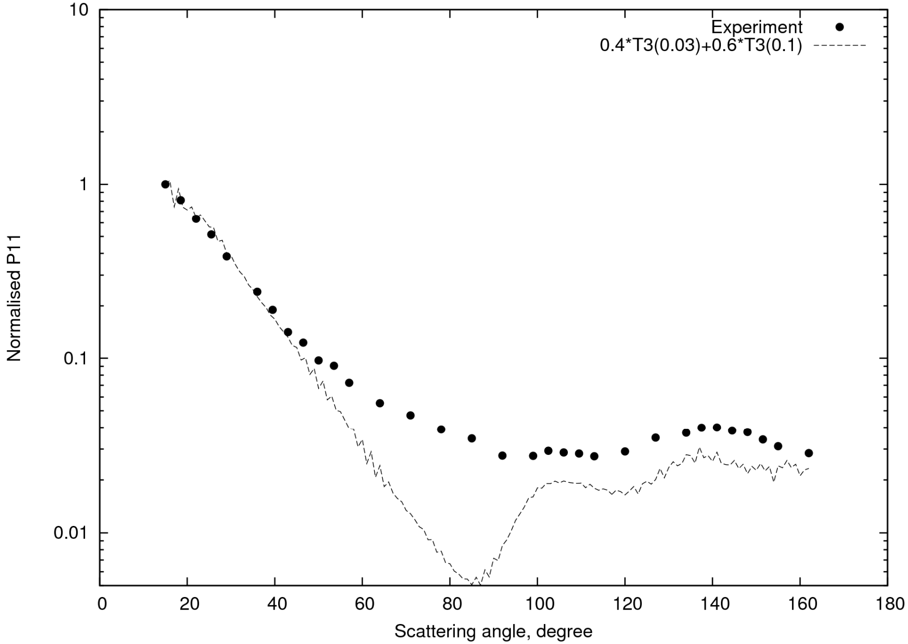

Fig. 2. The normalized scattering phase function plotted against the scattering angle. Showing, the PN measured average phase function (filled circles) and weighted habit mixture model 1 ($0.4 \times T3(0.03) + 0.6 \times T3(0.1)$), which is represented by the dashed line. The numbers in parenthesis are the assumed deformation parameters.

ACPD
12, 12485–12502, 2012

Unusual in-situ measured ice crystal scattering phase function

A. J. Baran et al.

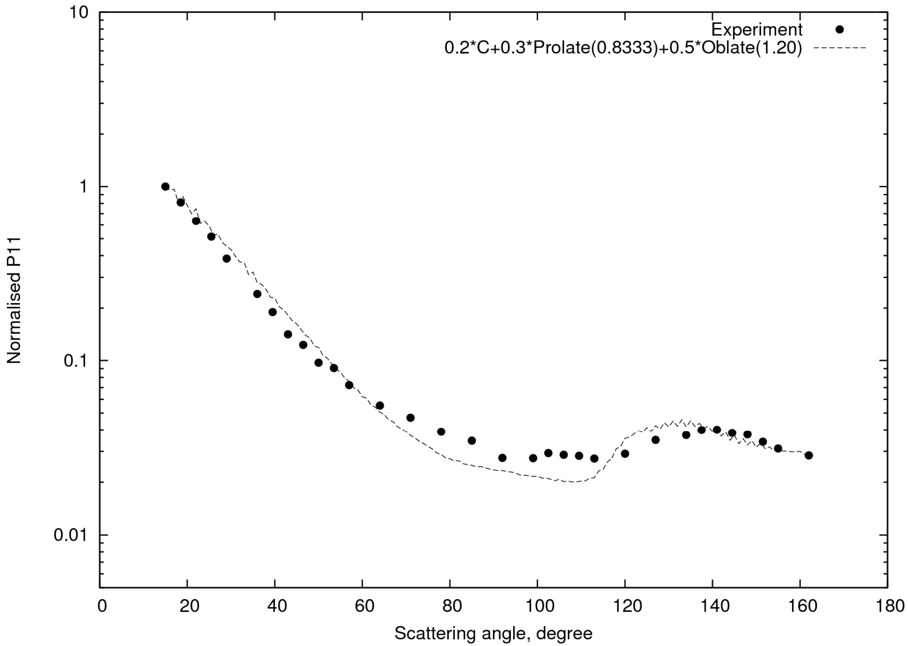

Fig. 3. Same as Fig. 2, but for the weighted habit mixture model 2, $0.2 \times C + 0.3 \times \text{Prolate}(0.8333) + 0.5 \times \text{Oblate}(1.2)$, where C represents the ten element hexagonal ice aggregate. The numbers in parenthesis are the assumed aspect ratios.

ACPD
12, 12485–12502, 2012

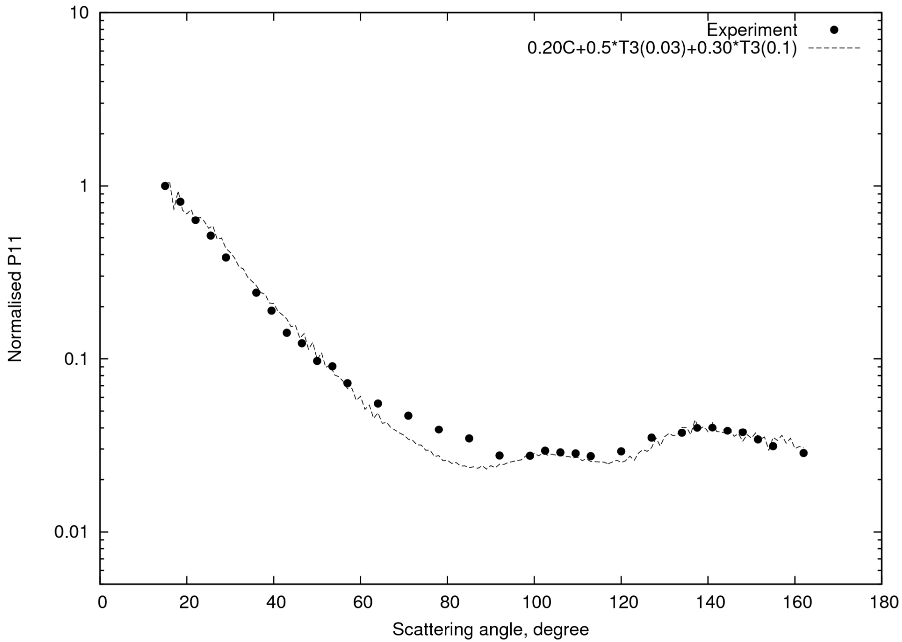

Fig. 4. Same as Fig. 3, but for weighted habit mixture model 3, $0.2 \times C + 0.5 \times T3(0.03) + 0.3 \times T3(0.1)$.

ACPD
12, 12485–12502, 2012